Hooker, J. A. Miller, *J. Hum. Evol.* **10**, 49 (1981).
8. M. Pickford, *Muench. Geowiss. Abh.* **8** (1986), 151 pp.
9. G. D. Thackray, thesis, University of Oregon, Eugene (1989).
10. Since 1984, our studies have characterized 95 paleosols of 20 kinds from Koru, Songhor, Rusinga Island, and Fort Ternan, ranging in geological age from 12 to 20 million years.
11. Date corrected to new constants by the procedure of G. B. Dalrymple [*Geology (Boulder)* 7, 558 (1979)].
12. Floor area 132 m^2, wall length 46 m, and wall area about 165 m^2.
13. Colors compared with a Munsell chart; grain size distribution and petrographic composition determined from 500 points in thin section with a Swift automatic point counter; G. S. Smith counted Onuria and Dhero paleosols of Fig. 1, and G.J.R. confirmed Onuria and counted Chogo paleosols; organic carbon by D. A. Horneck, Soil Testing Laboratory of Oregon State University, with the Walkley-Black technique; chemical analyses from Atomic Absorption by C. McBirney, University of Oregon.
14. Terminology of Soil Survey Staff, *Handb. U.S. Dep. Agric. 436* (1975).
15. F. J. Stevenson, *Soil Sci.* **107**, 470 (1969).
16. Burial by 600 m was estimated from a reconstruction of Tinderet volcano by analogy with the petrologically similar nearby volcano Kisingiri, studied by M. J. Le Bas [*Carbonatite-Nephelinite Volcanism* (Wiley, London, 1977)] and compaction from standard curve of B. Baldwin and C. O. Butler [*Bull. Am. Assoc. Petrol. Geol.* **69**, 622 (1985)].
17. H. A. de Wit, *Soils and Grassland Types of the Serengeti Plain (Tanzania)*, (Mededelingen Landbouwhogeschool Wageningen, the Netherlands, 1978); G. D. Anderson and L. W. Talbot, *J. Ecol.* **53**, 33 (1965).
18. T. J. Jager, *Soils of the Serengeti Woodlands, Tanzania* (Center for Agricultural Publishing and Documentation, Wageningen, the Netherlands, 1982).
19. C. Mizota, I. Kawasaki, T. Wakatsuki, *Geoderma* **43**, 131 (1988).
20. G. D. Anderson, *Sols Africains* **8**, 339 (1963); R. L. Hay, *J. Volcanol. Geotherm. Res.* **37**, 77 (1989).
21. R. L. Hay and R. J. Reeder, *Sedimentology* **25**, 649 (1978).
22. M. N. Machette, *Spec. Pap. Geol. Soc. Am. 302* (1985), p. 1.
23. P. L. Shipman, thesis, New York University (1977); R. Bonnefille, in *The Evolution of the East Asian Environment*, R. O. Whyte, Ed. (University of Hong Kong, Hong Kong, 1984), vol. 2, pp. 579–612.
24. D. A. Hooijer, *Zool. Meded. (Leiden)* **43**, 77 (1968); P. Tassy, *Bull. Soc. Geol. Fr.* **21**, 265 (1979).
25. H. Thomas, *Palaeogeogr. Palaeoclimatol. Palaeoecol.* **40**, 251 (1984); J. Kappelman, *Am. J. Phys. Anthropol.* **75**, 229 (1988).
26. M. Pickford, *J. Hum. Evol.* **14**, 113 (1985); *ibid.* **16**, 305 (1987).
27. H. Jenny, *Factors in Soil Formation* (McGraw-Hill, New York, 1941); R. J. Arkley, *Soil Sci.* **96**, 239 (1963); J. L. Sehgal, C. Sys, D. R. Bumbla, *Pedologie* **18**, 351 (1968).
28. D. P. Dugas, thesis, University of Oregon, Eugene (1989).
29. A set of 50 fossil grasses excavated in the laboratory from a single large oriented sandstone block had a vector mean orientation of 351° azimuth and a vector magnitude of 82% (a highly consistent orientation). Another set of 35 grasses measured in the field had a vector mean of 349° and a vector magnitude of 90%. In both sets the grasses dipped consistently to the north.
30. P. G. Palmer and A. E. Tucker, *Smithson. Contrib. Bot.* **49**, 1 (1981); *ibid.* **59**, 1 (1983); P. G. Palmer and S. Gerbeth-Jones, *ibid.* **62**, 1 (1986); *ibid.* **67**, 1 (1987); P. G. Palmer, S. Gerbeth-Jones, S. Hutchison, *ibid.* **55**, 1 (1985).
31. R. P. Ellis, in *Grass Systematics and Evolution*, T. R. Soderstrom, K. W. Hilu, C. S. Campbell, M. E. Barkworth, Eds. (Smithsonian Institution Press, Washington, DC, 1987), pp. 3–10.
32. B. F. Jacobs and C. A. S. Kabuye, *J. Hum. Evol.* **16**, 147 (1987).
33. C. R. Metcalfe, *Anatomy of the Monocotyledons* (Clarendon, Oxford, 1960).
34. C. M. Herrera, *Oikos* **45**, 446 (1985).
35. B. Senut, *Ann. Paleontol.* **74**, 128 (1988).
36. P. Andrews, M. Pickford, P. Shipman, and A. Walker helped with discussion; fieldwork was authorized by the Office of the President of the Republic of Kenya, under the auspices of the National Museums of Kenya and their director, R. E. Leakey; funded by the Wenner Gren Foundation and NSF grant EAR 8503232 to G.J.R., and by a Condon Award of the University of Oregon and Geological Society of America grants 3753-87 and 3969-88 to D.P.D.

26 June 1989; accepted 30 January 1990

Requirement for Activin A and Transforming Growth Factor–β1 Pro-Regions in Homodimer Assembly

ALANE M. GRAY AND ANTHONY J. MASON*

Many proteins are initially synthesized as part of a large precursor. The role of the pro-region in the biosynthesis of transforming growth factor–β1 (TGF-β1) and activin A, two structurally related disulfide-linked homodimers synthesized as large precursors, was studied. Vectors that expressed either the pro-region or the mature regions of these molecules were used in complementation experiments, only when the pro-region was coexpressed with the mature region did intracellular dimerization and secretion of biologically active homodimers occur. The pro-regions of activin A and TGF-β1, therefore, aid the folding, disulfide bond formation, and export of their respective homodimers.

ACTIVIN A AND TGF-β1 are members of a group of structurally related proteins that are involved in differentiation and have endocrine effects (*1*). This family consists of disulfide-linked homodimers derived from a large precursor that contains a hydrophobic signal sequence. The pro-regions of 290 (activin A) and 250 amino acids (TGF-β1) are linked by basic cleavage sites to the mature regions of 116 (activin A) and 112 amino acids (TGF-β1) (*2, 3*). We investigated the potential role of the pro-regions in the biosynthesis of both of these molecules.

Human 293S cells transfected with the expression plasmid pActA, which encodes the complete activin A precursor, secrete both a 25-kD disulfide-linked homodimer that comprises the COOH-terminal 116 amino acids of the activin A precursor and a protein of between 39.5 and 43.5 kD that corresponds to the activin A pro-region (*4*) (Fig. 1A and lanes 1 on Fig. 2, A and B). To independently express the pro-region and mature regions of the activin A precursor, we constructed the vectors pPTH-A and pProA (Fig. 1A). The vector pPTH-A, which contains the DNA sequence of the mature region of activin A fused in frame with a synthetic DNA sequence encoding the 31–amino acid prepro-region of human parathyroid hormone (PTH) (*5*) (Fig. 1B), was designed to determine whether the mature activin A sequences can fold correctly when expressed with a heterologous prepro-region. The prepro-PTH sequence has a well-characterized signal sequence and the six–amino acid basic pro-region is similar to

Department of Developmental Biology, Genentech, Inc., South San Francisco, CA 94080.

*To whom correspondence should be addressed.

Table 1. Bioactivity of activin A and TGF-β1 secreted from 293S cells. Serum-free conditioned medium (2.5 ml) was collected after 48 hours from confluent 60-mm dishes of transfected 293S cells. Bioactive activin A was measured in vitro by the induction of release of the pituitary hormone FSH from monolayers of rat pituitary cells (*9*). Conditioned media were assayed for FSH content by ELISA. Activin A was measured directly in conditioned media by a MAb-based ELISA. Data are averages of three experiments. Bioactive TGF-β1 was determined in a mink lung cell growth inhibition assay (*10*) after heat-activation of samples for 5 min at 75°C. TGF-β1 was measured by ELISA of conditioned medium after heat activation. UD, undetectable.

Plasmid	Activin A (ng/48 hours)		Plasmid	TGF-β1 (ng/48 hours)	
	Bioactive	ELISA		Bioactive	ELISA
Act A	950	730	TBF-β (SBβ)	1069	1190
PTH-A	UD	UD	PTH-TGF	2	UD
ProA	UD	UD	ProTGF	1	UD
PTH-A + ProA	83	65	PTH-TGF + ProTGF	25	26
Vector	UD	UD	Vector	3	UD

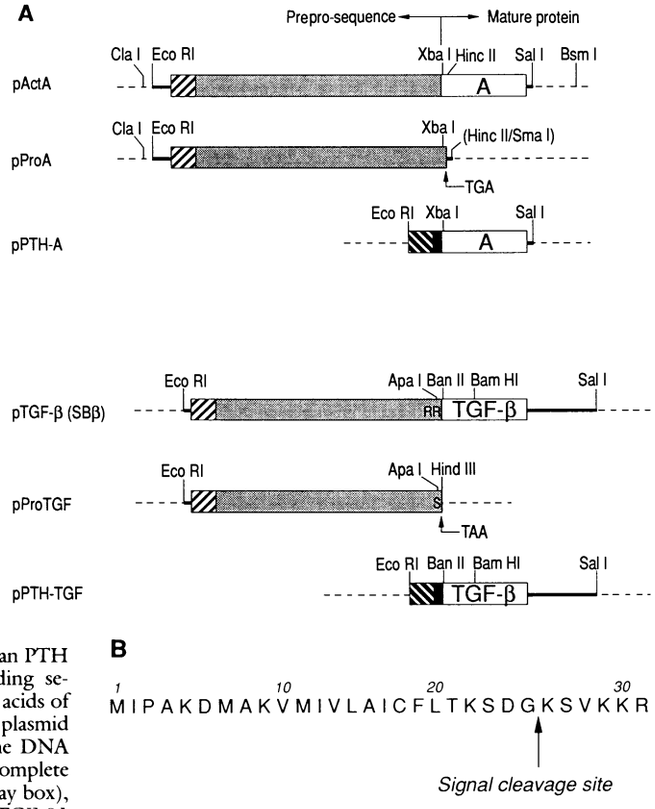

Fig. 1. (**A**) Schematic representation of the activin A and TGF-β1 coding regions contained in cytomegalovirus expression plasmids (*11*). The plasmid pActA contains the complete coding sequence for the activin A precursor, which consists of a presignal sequence (striped box), a pro-region (gray box), and a mature region (open box). The plasmid pProA contains the coding sequences for the prepro-region of the activin A precursor, and includes five consecutive Arg residues followed by an additional five amino acids before a TGA stop codon. Expression plasmid pPTH-A contains a synthetic DNA fragment encoding the pre- (striped box) and pro- (black box) regions of human PTH fused in frame to the coding sequences for the 116 amino acids of mature activin A. The plasmid pTGF-β (SBβ) contains the DNA sequence encoding the complete pre- (striped box), pro- (gray box), and mature regions of TGF-β1 (open box), whereas plasmid pProTGF contains the sequences for the prepro-region of TGF-β1 that terminates at Ser^{276}, which normally precedes the basic cleavage sites in the TGF-β1 precursor. The plasmid pPTH-TGF contains the mature sequences of TGF-β1 fused to the sequence encoding the prepro-region of human PTH. The positions of all restriction sites used for constructing these plasmids are represented by standard nomenclature. Plasmids were constructed with the use of standard techniques (*12*). (**B**) Protein sequence for the prepro-peptide of human PTH. The position at which the signal peptide is cleaved is represented by an arrow (*5*).

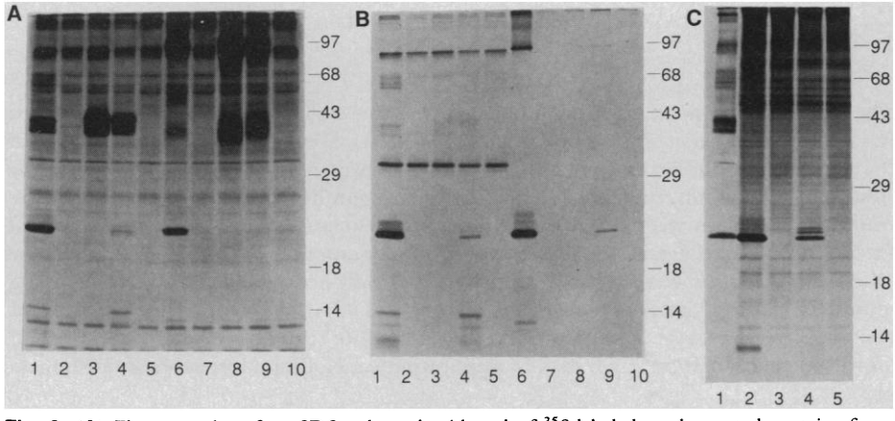

Fig. 2. (**A**) Fluorography of an SDS-polyacrylamide gel of ^{35}S-labeled total secreted proteins from transfected 293S cells. Lane 1, pActA; lane 2, pPTH-A; lane 3, pProA; lane 4, pPTH-A and pProA; lane 5, pRK5 vector control; lane 6, pTGF-β (SBβ); lane 7, pPTH-TGF; lane 8, pProTGF; lane 9, pPTH-TGF and pProTGF; and lane 10, pRK5 vector control. Molecular mass markers are indicated in kilodaltons. (**B**) Fluorography of an SDS-polyacrylamide gel of activin A and TGF-β1 immunoprecipitations. Lanes 1 to 5 are immunoprecipitations with an activin A polyclonal antibody (290B) of the same cell supernatants shown in (A), lanes 1 to 5. Lanes 6 to 10 are the samples shown in lanes 6 to 10 in (A) immunoprecipitated with TGF-β1–specific MAb 2G7. Molecular mass markers are indicated in kilodaltons (**C**) SDS-polyacrylamide gel of activin A MAb 309 immunoprecipitation of cell lysates. Lane 2, pActA cell lysate; lane 3, pPTH-A cell lysate; and lane 4, pPTH-A and pProA cell lysate. Lane 1 is total secreted proteins from pActA-transfected cells. Molecular mass markers are indicated in kilodaltons. DNA transfections of 293S cells (*13, 14*) metabolic labeling and immunoprecipitations were performed by standard techniques (*15*).

the five arginines in the activin A precursor at the junction between the pro- and mature regions. The plasmid pProA directs the expression of the prepro-region of the activin A precursor.

Cell supernatants from cells transfected with pPTH-A did not contain any detectable activin A monomers or dimers as judged by immunoprecipitation with a goat polyclonal antibody to activin A (290B) (Fig. 2B, lane 2). In contrast, the pro-region of the activin A precursor was secreted within 20 min when it was expressed independently of the mature region (Fig. 2A, lane 3) (6). Cells cotransfected with equimolar amounts of plasmid pPTH-A and pProA secreted small quantities of the 25-kD activin A dimer in addition to the activin pro-region (Fig. 2A, lane 4). The secreted dimer was recognized by activin A antibodies (Fig. 2B, lane 4) and was biologically active in an activin bioassay (Table 1). Quantification by both bioassay and ELISA show that pPTH-A plus pProA-transfected cells secreted ~9% of the activin A secreted from pActA-transfected cells (Table 1). Immunoprecipitation of cell lysates with a dimer-specific activin A monoclonal antibody (MAb 309) shows that dimerization occurred intracellularly in the pActA- and pPTH-A plus pProA-transfected cells (Fig. 2C, lanes 2 and 4), but no dimers were detected in pPTH-A cell lysates (Fig. 2C, lane 3). These data show that intracellular dimer formation was dependent on the presence of the activin A pro-molecule.

What is the fate of the activin A protein in pPTH-A–transfected cells? Because no specific proteins were precipitated from pPTH-A lysates in the presence of MAb 309 (Fig. 2C, lane 3), we attempted immunoprecipitations with the 290B polyclonal antiserum. Only when immunoprecipitations were reduced before electrophoresis was a prominent band ~1 kD larger than activin A monomer detected (*6*). This indicates that activin A monomers synthesized in pPTH-A–transfected cells are translocated successfully, retain the six–amino acid pro-PTH sequence, and form large disulfide-linked aggregates either with themselves or other proteins. Activin A disulfide-linked aggregates were also present in cells transfected with both pPTH-A and pProA, suggesting that activin A monomers unable to interact with a pro-region molecule aggregate in the endoplasmic reticulum (*6*).

To establish whether these results could be extended to other members of the TGF-β superfamily, we constructed a similar set of expression vectors using the coding sequences for the TGF-β1 precursor (Fig. 1A). Analogous transfection experiments with these plasmids showed that, whereas

no TGF-β1 dimers are secreted from cells transfected with the plasmid pPTH-TGF (Fig. 2B, lane 7), cotransfection of pPTH-TGF and pProTGF results in secretion of biologically active TGF-β1 dimers (Fig. 2B, lane 9, and Table 1). As judged by bioactivity and ELISA, ~2.4% of the amount of TGF-β1 present in supernatants from pTGF-β–transfected cells was present in supernatants from pPTH-TGF and pProTGF-transfected cells (Table 1). The reasons for the lower efficiency of dimer rescue by the proTGF-β sequence as compared with the results obtained with the activin A constructions are not understood.

No activin A dimers were secreted from cells transfected with pPTH-A and pProTGF, but activin A dimers were detected in transfection experiments with a vector containing the proTGF-β1 sequences fused to the mature activin A sequences (*6*). It would therefore appear that the proTGF-β1 sequences can substitute, albeit at a low efficiency, for the activin A pro-sequences. This result suggests that sequences in the pro-region responsible for mature region–pro-region interaction may be conserved between activin A and TGF-β1. The pro-region of TGF-β1 has been shown to contain one or more binding sites for the mature homodimers since the pro-regions and mature regions are secreted from cells as a large noncovalently linked latent complex (*7*). It is tempting to speculate that the binding site or sites responsible for the formation of the TGF-β1 noncovalent complex are also used by the pro-region as it aids the dimerization of the mature regions.

The results of the complementation experiments presented here demonstrate that the pro-regions of activin A and TGF-β1 are essential for the folding and assembly of activin A and TGF-β1 dimers. The ability of an independently expressed pro-region to aid in the folding of a mature protein has been previously reported for a number of proteases (*8*).

REFERENCES AND NOTES

1. J. Massagué, *Cell* **49**, 437 (1987).
2. A. J. Mason *et al.*, *Nature* **318**, 659 (1985).
3. R. Derynck *et al.*, *ibid.* **316**, 701 (1985).
4. R. H. Schwall, K. Nikolics, E. Szonyi, C. Gorman, A. J. Mason, *Mol. Endocrinol.* **3**, 1237 (1988).
5. G. N. Hendy, H. M. Kronenberg, J. T. Potts, Jr., A. Rich, *Proc. Natl. Acad. Sci. U.S.A.* **78**, 7365 (1981).
6. A. M. Gray and A. J. Mason, unpublished data.
7. L. E. Gentry, M. N. Liubin, A. F. Purchio, H. Marquardt, *Mol. Cell. Biol.* **8**, 4162 (1988); K. Miyazono, V. Hellman, C. Wernstadt, C.-H. Heldin, *J. Biol. Chem.* **263**, 7646 (1988).
8. X. Zhu, Y. Ohta, F. Jordan, M. Inouye, *Nature* **339**, 483 (1989); J. L. Silen and D. A. Agard, *ibid.* **341**, 462 (1989).
9. W. Vale, G. Grant, M. Amoss, R. Blackwell, R. Guillemin, *Endocrinology* **91**, 562 (1972).
10. L. M. Wakefield, D. M. Smith, K. C. Flanders, M. B. Sporn, *J. Biol. Chem.* **263**, 7646 (1988).
11. C. M. Gorman, D. R. Gies, G. McCray, *DNA-Protein Eng.* **2**, 1 (1990).
12. The sequences coding for the mature activin A subunit in pActA were assembled from synthetic oligonucleotides, a procedure that introduced unique restriction sites but conserved the protein sequence. pProA: To express the prepro-polypeptide of the activin A precursor, a stop codon was introduced in pActA. The Xba I site was filled in generating a stop codon five amino acids downstream from the basic processing site of the propeptide and creating the sequence Gly-Leu-Ala-Arg-Val after Arg^{282}. The Cla I–Hinc II fragment was then recloned into the vector RKB that had been cut with Cla I and Sma I. pPTH-A: A synthetic 113-bp Eco RI–Xba I fragment encoding the PTH prepro-polypeptide fused to the first three bases of mature activin A sequences was ligated into the plasmid pActA that had been cut with Eco RI and Xba I, replacing the βA prepro-sequences. pProTGF: A stop codon was introduced after Ser^{276} of the TGF-β propeptide, deleting the basic cleavage site, by ligation of a synthetic 21-bp Apa I–Hind II fragment and the 817-bp Eco RI–Apa I fragment from pTGF-β into the vector pRK5 that had been cut with Eco RI and Hind II. pPTH-TGF: A synthetic 113-bp Eco RI–Ban II fragment encoding the PTH prepro-polypeptide fused to the first three bases of mature TGF-β sequences was ligated along with the 96-bp Ban II–Bam HI fragment from pTGF-β into the plasmid pTGF-β that had been cut with Eco RI and Bam HI.
13. F. L. Graham and A. J. van der Eb, *Virology* **52**, 456 (1973).
14. C. Gorman, R. Padmanabhan, B. H. Howard, *Science* **221**, 551 (1983).
15. Human 293S cells seeded at ~30% confluency in 60-mm dishes were transfected the following day with 2.5 μg of each plasmid DNA and 2 μg of plasmid encoding the SV40 T-antigen and the Rous sarcoma virus promoter. The next day cells were labeled in 1.0 ml of serum-free Dulbecco's minimum essential medium with [^{35}S]cysteine and [^{35}S]methionine (250 μCi/ml each) for 1 to 2 hours. Labeling medium was removed, and secreted proteins were collected for 4 to 5 hours in 1 ml of serum-free medium. The supernatant was cleared by centrifugation, and rinsed cells were lysed in 0.5 ml of lysis buffer (1% NP-40, 0.5% deoxycholate, 0.1% SDS; and 5 m*M* EDTA in phosphate-buffered saline) and spun for 10 min, and the lysate was frozen until use. Secreted proteins (100 μl) were immunoprecipitated with either polyclonal antibody 290B, an antibody to recombinant human activin A dimer that recognizes both dimer and monomer (and displays some cross-reaction with the activin A precursor sequences), or mouse MAb 2G7 to recombinant human TGF-β. Cell lysates were immunoprecipitated with MAb 309, which recognizes only activin A dimer. Supernatants to be precipitated with the TGF-β antibody were heated at 75°C for 5 min in the presence of 0.1% bovine serum albumin and chilled on ice before addition of antibody. Immune complexes of secreted proteins were precipitated with Pansorbin (Calbiochem) and cell lysates, with protein A–Sepharose (Pharmacia). Denatured immunoprecipitates or total secreted proteins (15 μl) were separated by electrophoresis on 13% SDS-polyacrylamide gels and were permeated with Enhance (Du Pont) and exposed for 3 days at −70°C.

16. We thank A. Evans for critical comments on this manuscript; A. Levinson and S. Broz for supplying the plasmid pTGF-β (SBβ); H. Niall for the suggestion of using the prepro-region of PTH; and R. Schwall, W.-L. Wong, J. Lofgren, L. Bald, and members of the Genentech assay group for assistance. Synthetic oligonucleotides were made by P. Ng, M. Vasser, and P. Jhurani of the Genentech DNA synthesis group.

10 October 1989; accepted 12 January 1990

Imaging and Manipulating Molecules on a Zeolite Surface with an Atomic Force Microscope

A. L. WEISENHORN, J. E. MAC DOUGALL, S. A. C. GOULD, S. D. COX, W. S. WISE, J. MASSIE, P. MAIVALD, V. B. ELINGS, G. D. STUCKY, P. K. HANSMA

The adsorption of neutral molecules and ions on the surfaces of zeolites was observed in real time with an atomic force microscope (AFM). Direct imaging of the surface of the zeolite clinoptilolite was possible by using a diluted *tert*-butyl ammonium chloride solution as a medium. Images of the crystal in different liquids revealed that molecules could be bound to the surface in different ways; neutral molecules of *tert*-butanol formed an ordered array, whereas *tert*-butyl ammonium ions formed clusters. These absorbed molecules were not rearranged by the AFM tip when used in an imaging mode. However, when a sufficiently large force was applied, the tip of the AFM could rearrange the *tert*-butyl ammonium ions on the zeolite surface. This demonstration of molecular manipulation suggests new applications, including biosensors and lithography.

ZEOLITES ARE CRYSTALLINE ALUminosilicates that have a regular pore or channel structure on the order of atomic dimensions (*1*). Introducing aluminum atoms into a silica network yields a negative charge per Al atom so that cations are required to balance the charge. These cations are loosely bound to framework oxygen atoms and can be readily exchanged for other cations in most cases. Zeolites with the appropriate combination of molecularly sized holes and cation exchange ability have found a great number of uses in the chemical industry. For example, acid zeolite Y catalysts are used to crack crude oil (*2*), ZSM-5 (a high silica content zeolite) is used to convert methanol to gasoline (*3*), zeolite A is used as a water softener in homes (*4*), and clinoptilolite is used for waste-water treatment to remove ammonium and phosphate